Inorg. Chem. **2005**, *44*, 727−741

Forum

Spectroscopic Approaches to Elucidating Novel Iron−Sulfur Chemistry in the "Radical-SAM" Protein Superfamily

Charles J. Walsby,[†,‡] Danilo Ortillo,[§] Jian Yang,[§] Mbako R. Nnyepi,[§] William E. Broderick,[§] Brian M. Hoffman,[‡] and Joan B. Broderick*[,§]

Departments of Chemistry, Michigan State University, East Lansing, Michigan 48824, Simon Fraser University, Burnaby, BC, V5A 1S6 Canada, and Northwestern University, Evanston, Illinois 60208

Received October 29, 2004

Electron paramagnetic resonance (EPR), electron–nuclear double resonance (ENDOR), and Mössbauer spectroscopies and other physical methods have provided important new insights into the radical-SAM superfamily of proteins, which use iron–sulfur clusters and *S*-adenosylmethionine to initiate H atom abstraction reactions. This remarkable chemistry involves the generation of the extremely reactive 5′-deoxyadenosyl radical, the same radical intermediate utilized in B_{12}-dependent reactions. Although early speculation focused on the possibility of an organometallic intermediate in radical-SAM reactions, current evidence points to novel chemistry involving a site-differentiated [4Fe–4S] cluster. The focus of this forum article is on one member of the radical-SAM superfamily, pyruvate formate-lyase activating enzyme, and how physical methods, primarily EPR and ENDOR spectroscopies, are contributing to our understanding of its structure and mechanism. New ENDOR data supporting coordination of the methionine moiety of SAM to the unique site of the $[4Fe–4S]^{2+/+}$ cluster are presented.

Introduction

Iron−sulfur clusters are among the most ubiquitous and versatile metal centers found in biological systems. Both [2Fe−2S] and [4Fe−4S] clusters serve as electron-transfer centers in such central biological functions as photosynthesis and respiration, and it is the broadly tuneable redox potentials of these clusters, mediated by the coordination environment, the surrounding protein milieu, and hydrogen bonding, that defines their versatility. Electron transfer was the first function recognized for iron−sulfur clusters in biology; however, there has been dramatically renewed interest in these clusters as a result of discoveries of both novel functions and novel structures.[1,2] Among the novel functions, iron−sulfur clusters are directly involved in catalyzing reactions occurring at enzyme active sites. Perhaps the best known example of an enzyme using a catalytic iron−sulfur cluster is aconitase, an enzyme in the citric acid cycle that catalyzes the dehydration/hydration reactions involved in converting citrate to isocitrate; aconitase uses a site-differentiated [4Fe−4S] cluster as a Lewis acid in this reaction.[3,4] Several other dehydratases utilizing iron−sulfur clusters as Lewis acids are also known.[5] Among the more complex enzymes using a catalytic iron−sulfur cluster is nitrogenase, in which a complex Mo−Fe−S cluster binds and activates N_2 for reduction by a mechanism that is still not well understood.[6,7] The nitrogenase MoFe cofactor is also

* To whom correspondence should be addressed. E-mail: broderij@cem.msu.edu.
† Simon Fraser University.
‡ Northwestern University.
§ Michigan State University.

(1) Beinert, H.; Holm, R. H.; Münck, E. *Science* **1997**, *277*, 653−659.
(2) Beinert, H. *J. Biol. Inorg. Chem.* **2000**, *5*, 2−15.
(3) Beinert, H.; Kennedy, M. C.; Stout, C. D. *Chem. Rev.* **1996**, *96*, 2335−2373.
(4) Broderick, J. B. In *Comprehensive Coordination Chemistry II*; McCleverty, J. A., Meyer, T. J., Eds.; Elsevier Ltd.: Oxford, U.K., 2004; Vol. 8, pp 739−757.
(5) Flint, D. H.; Allen, R. M. *Chem. Rev.* **1996**, *96*, 2315−2334.
(6) Holland, P. L. In *Comprehensive Coordination Chemistry II*; McCleverty, J. A., Meyer, T. J., Eds.; Elsevier Ltd.: Oxford, U.K., 2004; Vol. 8, pp 569−599.
(7) Igarashi, R. Y.; Seefeldt, L. C. *Crit. Rev. Biochem. Mol. Biol.* **2003**, *38*, 351−384.

10.1021/ic0484811 CCC: $30.25
Published on Web 01/22/2005

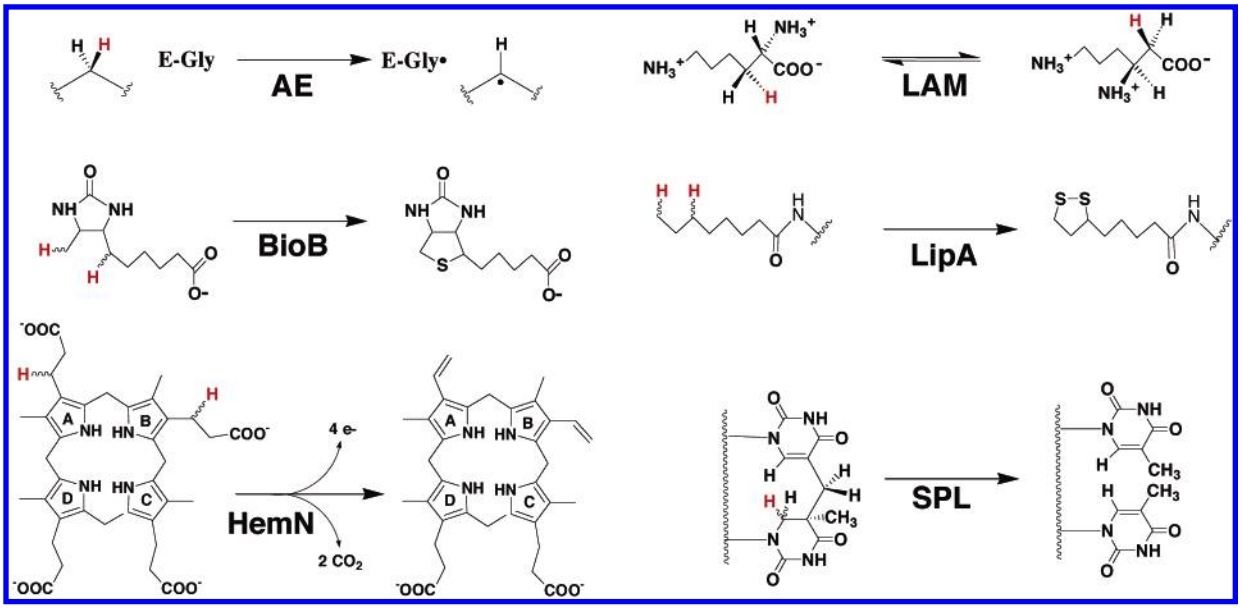

Figure 1. Reactions catalyzed by representative members of the radical-SAM superfamily. AE, activating enzymes; LAM, lysine 2,3-aminomutase; BioB, biotin synthase; LipA, lipoate synthase; HemN, oxygen-independent coproporphyrinogen III synthase; SPL, spore photoproduct lyase.

a good example of a cluster with a novel structure, in essence two fused partial cubane clusters with a nitride occupying the center.[8] The acetyl-CoA synthase (ACS)/carbon monoxide dehydrogenase (CODH) enzymes provide another interesting enzymatic example of novel iron−sulfur cluster structures and chemistry.[9,10] Recent crystal structures of ACS and CODH enzymes reveal two novel clusters: a C cluster with an unusual [$NiFe_4S_5$] structure[11,12] and an A cluster in which an [Fe_4S_4] cluster is bridged to a binuclear metal center containing nickel.[13,14] The former cluster is involved in catalyzing the reversible reduction of CO_2, whereas the latter is involved in the synthesis of acetyl-coenzyme A from CO. As is the case with nitrogenase, the details of the mechanism of ACS/CODH and the precise role of the iron−sulfur cluster in catalysis are subjects of active investigation.

The "Radical-SAM" Superfamily. The reactions catalyzed by the "radical-SAM" superfamily of proteins provide yet another example of novel chemistry for iron−sulfur clusters. These enzymes use an iron−sulfur cluster and *S*-adenosylmethionine (SAM or AdoMet) to catalyze diverse radical chemistry on a vast array of substrates.[15−19] The superfamily was first identified in 2001 and is thought to contain more than 600 members present in organisms as diverse as microbes and humans;[20] therefore, this superfamily represents a large new class of iron−sulfur proteins. Although little is known about most members of this superfamily, several have been under investigation since well before the superfamily was named and have provided new insights into the role of the iron−sulfur cluster in initiating radical catalysis. Some of the reactions known to be catalyzed by members of the radical-SAM superfamily are shown in Figure 1. The remarkable diversity of these reactions is readily apparent, and yet our current thinking is that all of these reactions, as well as those radical-SAM reactions yet undiscovered, involve a common mechanism. The key initial reaction of the substrate in each of the reactions shown in Figure 1 is hydrogen atom abstraction: in all cases, the indicated C−H bond cleavage must be achieved. Mechanistically, therefore, the question is how *S*-adenosylmethionine can be used to initiate a H atom abstraction reaction.

***S*-Adenosylmethionine as a Cofactor.** *S*-Adenosylmethionine plays a number of important roles in living organisms, including transmethylation, trans-sulfuration, and polyamine biosynthesis.[21,22] Methyl group donation is the most recognized function of this molecule and involves heterolytic cleavage of the S−C bond such that a methyl cation is the donated species. In the radical-SAM enzymes, however, evidence points to homolytic S−C bond cleavage in *S*-adenosylmethionine as a source of 5′-deoxyadenosyl radicals, which perform the key hydrogen atom abstraction

(8) Einsle, O.; Tezcan, F. A.; Andrade, S. L. A.; Schmid, B.; Yoshida, M.; Howard, J. B.; Rees, D. C. *Science* **2002**, *297*, 1696−1700.
(9) Drennan, C. L.; Peters, J. W. *Curr. Opin. Struct. Biol.* **2003**, *13*, 220−226.
(10) Drennan, C. L.; Doukov, T. I.; Ragsdale, S. W. *J. Biol. Inorg. Chem.* **2004**, *9*, 511−515.
(11) Drennan, C. L.; Heo, J.; Sintchak, M. D.; Schreiter, E.; Ludden, P. W. *Proc. Natl. Acad. Sci. U.S.A.* **2001**, *98*, 11973−11978.
(12) Dobbek, H.; Svetlitchnyi, V.; Gremer, L.; Huber, R.; Meyer, O. *Science* **2001**, *293*, 1281−1285.
(13) Doukov, T. I.; Iverson, T. M.; Seravalli, J.; Ragsdale, S. W.; Drennan, C. L. *Science* **2002**, *298*, 567−572.
(14) Darnault, C.; Volbeda, A.; Kim, E. J.; Legrand, P.; Vernede, X.; Lindahl, P. A.; Fontecilla-Camps, J. C. *Nat. Struct. Biol.* **2003**, *10*, 271−279.
(15) Cheek, J.; Broderick, J. B. *J. Biol. Inorg. Chem.* **2001**, *6*, 209−226.
(16) Fontecave, M.; Mulliez, E.; Ollagnier-de-Choudens, S. *Curr. Opin. Chem. Biol.* **2001**, *5*, 506−511.
(17) Broderick, J. B. In *Comprehensive Coordination Chemistry II: From Biology to Nanotechnology*; McCleverty, J., Meyer, T. J., Que, L., Tolman, W. B., Eds.; Elsevier: Oxford, U.K., 2003; Vol. 8, pp 739−757.
(18) Jarrett, J. T. *Curr. Opin. Chem. Biol.* **2003**, *7*, 174−182.
(19) Frey, P. A.; Magnusson, O. T. *Chem. Rev.* **2003**, *103*, 2129−2148.
(20) Sofia, H. J.; Chen, G.; Hetzler, B. G.; Reyes-Spindola, J. F.; Miller, N. E. *Nucleic Acids Res.* **2001**, *29*, 1097−1106.
(21) Markham, G. D. In *Nature Encyclopedia of Life Sciences*; Nature Publishing Group: London, 2002.
(22) Fontecave, M.; Atta, M.; Mulliez, E. *Trends Biochem. Sci.* **2004**, *29*, 243−249.

noted above. This role for *S*-adenosylmethionine was completely unprecedented at the time it was first proposed.[23,24] In fact, at that time, only adenosylcobalamin (B_{12}) was known to generate 5′-deoxyadenosyl radicals in biology. The B_{12} cofactor, with its relatively weak Co−C bond, is believed to undergo Co−C bond homolysis to produce cob(II)alamin and an adenosyl radical, with the energy for homolysis provided, in part, by the binding interactions of the cofactor and substrate to the enzyme.[25,26] How a relatively simple molecule such as *S*-adenosylmethionine, which has only the adenosyl moiety in common with B_{12}, could produce the same highly reactive primary radical intermediate was a perplexing question. Because both lysine 2,3-aminomutase and pyruvate formate-lyase activating enzyme, two of the earliest-studied radical-SAM enzymes, were reported to require metals for catalysis,[27−30] significant speculation surrounded the possibility of organometallic intermediates involving metal−adenosyl complexes.[23,31] As will be discussed further, however, the radical-SAM enzymes appear to use a completely unprecedented mechanism for generating the extremely reactive 5′-deoxyadenosyl radical intermediate.

Functional Insight from Electron Paramagnetic Resonance Spectroscopy and other Physical Methods. Electron paramagnetic resonance (EPR) spectroscopy has been central to the developing understanding of the radical-SAM enzymes. As detailed in the next section, it was EPR spectroscopy that first demonstrated the presence of a stable glycyl radical in pyruvate formate lyase,[23,32] and EPR has now been used to identify glycyl radicals in other enzymes, including the anaerobic ribonucleotide reductase[33] and benzylsuccinate synthase,[34] that are substrates of radical-SAM activating enzymes. EPR spectroscopy has also played a key role in identifying iron−sulfur clusters in radical-SAM enzymes and, together with Mössbauer spectroscopy, in characterizing cluster types and oxidation states and identifying the catalytically active cluster.[29,33,35−46] Electron−nuclear double resonance (ENDOR) spectroscopy, which probes coupling between electronic and nuclear spins,[47] provided the first evidence for the close proximity of SAM to the iron−sulfur cluster, as well as for direct coordination of the unique iron site of the iron−sulfur cluster by SAM.[48,49] This unprecedented structural motif, with the amino and carboxylate moieties of SAM coordinating the unique iron site of a [4Fe−4S] cluster, appears to be a key element of radical-SAM enzyme function, as it has now appeared in crystal structures of three diverse members of the radical-SAM superfamily.[50−52] In addition to this novel coordination mode, ENDOR spectroscopy provided evidence for direct orbital overlap between the sulfonium of SAM and the iron−sulfur cluster, a feature of the SAM-cluster interaction that is not apparent in the X-ray crystal structures but is indisputable based on the ENDOR data.[48] EPR and ENDOR spectroscopies have clearly been central to the development of understanding of the radical-SAM enzymes, and have more than once been the basis for radical new ways of thinking about these fascinating enzymes, as will be discussed in further detail in following sections.

Pyruvate Formate-Lyase: The First-Identified Glycyl Radical Enzyme.

Pyruvate formate-lyase (PFL), an enzyme involved in anaerobic glucose metabolism in *Escherichia coli* and other facultative anaerobes, has the distinction of being the first enzyme ever identified to contain a stable and catalytically essential glycyl radical.[23,32,53] This remarkable discovery was made using electron paramagnetic resonance (EPR) spectroscopy in combination with isotopic labeling, together with analysis of the products of oxygenolytic cleavage of the radical-containing protein. The identification of a catalytically essential glycyl radical in pyruvate formate-lyase raised three key questions: (1) What is the mechanism by which a glycyl

(23) Knappe, J.; Neugebauer, F. A.; Blaschkowski, H. P.; Gänzler, M. *Proc. Natl. Acad. Sci U.S.A.* **1984**, *81*, 1332−1335.
(24) Moss, M.; Frey, P. A. *J. Biol. Chem.* **1987**, *262*, 14859−14862.
(25) Banerjee, R., Ed. *Chemistry and Biochemistry of B12*; Wiley-Interscience: New York, 1999.
(26) Banerjee, R. *Biochemistry* **2001**, *40*, 6191−6198.
(27) Chirpich, T. P.; Zappia, V.; Costilow, R. N.; Barker, H. A. *J. Biol. Chem.* **1970**, *245*, 1778−1789.
(28) Song, K. B.; Frey, P. A. *J. Biol. Chem.* **1991**, *266*, 7651−7655.
(29) Petrovich, R. M.; Ruzicka, F. J.; Reed, G. H.; Frey, P. A. *J. Biol. Chem.* **1991**, *266*, 7656−7660.
(30) Conradt, H.; Hohmann-Berger, M.; Hohmann, H.-P.; Blaschkowski, H. P.; Knappe, J. *Arch. Biochem. Biophys.* **1984**, *228*, 133−142.
(31) Frey, P. A. *FASEB J.* **1993**, *7*, 662−670.
(32) Wagner, A. F. V.; Frey, M.; Neugebauer, F. A.; Schäfer, W.; Knappe, J. *Proc. Natl. Acad. Sci. U.S.A.* **1992**, *89*, 996−1000.
(33) Mulliez, E.; Fontecave, M.; Gaillard, J.; Reichard, P. *J. Biol. Chem.* **1993**, *268*, 2296−2299.
(34) Krieger, C. J.; Roseboom, W.; Albracht, S. P. J.; Spormann, A. M. *J. Biol. Chem.* **2001**, *276*, 12924−12927.
(35) Broderick, J. B.; Duderstadt, R. E.; Fernandez, D. C.; Wojtuszewski, K.; Henshaw, T. F.; Johnson, M. K. *J. Am. Chem. Soc.* **1997**, *119*, 7396−7397.
(36) Külzer, R.; Pils, T.; Kappl, R.; Hüttermann, J.; Knappe, J. *J. Biol. Chem.* **1998**, *273*, 4897−4903.
(37) Broderick, J. B.; Henshaw, T. F.; Cheek, J.; Wojtuszewski, K.; Trojan, M. R.; McGhan, R.; Smith, S. R.; Kopf, A.; Kibbey, M.; Broderick, W. E. *Biochem. Biophys. Res. Commun.* **2000**, *269*, 451−456.
(38) Krebs, C.; Henshaw, T. F.; Cheek, J.; Huynh, B.-H.; Broderick, J. B. *J. Am. Chem. Soc.* **2000**, *122*, 12497−12506.
(39) Petrovich, R. M.; Ruzicka, F. J.; Reed, G. H.; Frey, P. A. *Biochemistry* **1992**, *31*, 10774−10781.
(40) Lieder, K.; Booker, S.; Ruzicka, F. J.; Beinert, H.; Reed, G. H.; Frey, P. A. *Biochemistry* **1998**, *37*, 2578−2585.
(41) Liu, A.; Gräslund, A. *J. Biol. Chem.* **2000**, *275*, 12367−12373.
(42) Ollagnier, S.; Meier, C.; Mulliez, E.; Gaillard, J.; Schuenemann, V.; Trautwein, A.; Mattioli, T.; Lutz, M.; Fontecave, M. *J. Am. Chem. Soc.* **1999**, *121*, 6344−6350.
(43) Tamarit, J.; Mulliez, E.; Meier, C.; Trautwein, A.; Fontecave, M. *J. Biol. Chem.* **1999**, *274*, 31291−31296.
(44) Ollagnier, S.; Mulliez, E.; Schmidt, P. P.; Eliasson, R.; Gaillard, J.; Deronzier, C.; Bergman, T.; Gräslund, A.; Reichard, P.; Fontecave, M. *J. Biol. Chem.* **1997**, *272*, 24216−24223.
(45) Ollagnier, S.; Mulliez, E.; Gaillard, J.; Eliasson, R.; Fontecave, M.; Reichard, P. *J. Biol. Chem.* **1996**, *271*, 9410−9416.
(46) Henshaw, T. F.; Cheek, J.; Broderick, J. B. *J. Am. Chem. Soc.* **2000**, *122*, 8331−8332.
(47) Hoffman, B. M. *Acc. Chem. Res.* **2003**, *36*, 522−529.
(48) Walsby, C. J.; Hong, W.; Broderick, W. E.; Cheek, J.; Ortillo, D.; Broderick, J. B.; Hoffman, B. M. *J. Am. Chem. Soc.* **2002**, *124*, 3143−3151.
(49) Walsby, C. J.; Ortillo, D.; Broderick, W. E.; Broderick, J. B.; Hoffman, B. M. *J. Am. Chem. Soc.* **2002**, *124*, 11270−11271.
(50) Layer, G.; Moser, J.; Heinz, D. W.; Jahn, D.; Schubert, W.-D. *EMBO J.* **2003**, *22*, 6214−6224.
(51) Berkovitch, F.; Nicolet, Y.; Wan, J. T.; Jarrett, J. T.; Drennan, C. L. *Science* **2004**, *303*, 76−79.
(52) Hänzelmann, P.; Schindelin, H. *Proc. Natl. Acad. Sci. U.S.A.* **2004**, *101*, 12870−12875.
(53) Unkrig, V.; Neugebauer, F. A.; Knappe, J. *Eur. J. Biochem.* **1989**, *184*, 723−728.

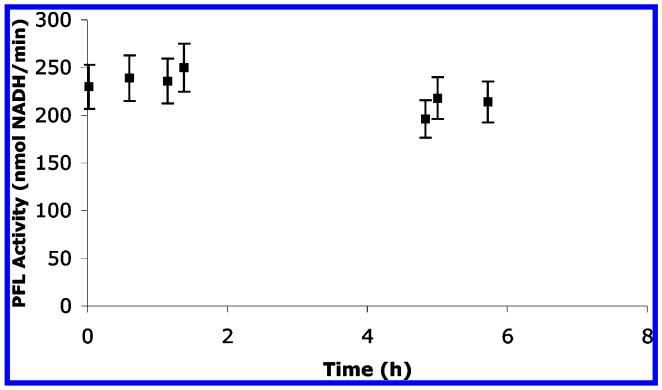

Figure 2. Plot of residual PFL activity as a function of time of incubation at 25 °C under anaerobic conditions. The PFL activity is a reflection of the presence of the catalytically essential glycyl radical. Analogous experiments in which the EPR signal of the glycyl radical is monitored over time provide identical results (data not shown).

radical mediates the C−C bond cleavage reaction of converting pyruvate to formate, (2) what is responsible for the unusual stability of the glycyl radical, and (3) how is the glycyl radical generated? The first question has been the subject of active investigation for nearly 30 years, and yet uncertainty remains regarding the precise role of the glycyl radical in catalysis.

The stability of the glycyl radical is truly remarkable. The half-life of the PFL glycyl radical under anaerobic conditions and at 30 °C was previously reported to be several hours.[53,54] However, in our laboratory, both the PFL catalytic activity and the glycyl radical EPR signal were found to be retained for days at 30 °C in an anaerobic glovebox (Figure 2); we have estimated the half-life under these conditions to be *at least* 24 h. The "capto-dative" effect,[55] the combined stabilization resulting from an adjacent electron donor (the amide nitrogen) on one side of the glycyl radical and an electron acceptor (the carbonyl of the next amide bond) on the other side, has been invoked to explain the stability of the glycyl radical.[56] However, more recently, the synergistic capto-dative effect for α-carbon-centered peptide radicals has been refuted in both peptide model studies[57] and density functional theory studies,[58] both of which show only additive, not synergistic, stabilization effects of the adjacent amide and carbonyl groups in the protein-bound glycyl radical. The X-ray crystal structure of PFL also sheds some light on the glycyl radical stability, as the radical site (glycine 734) is buried within the protein structure and thus should be less accessible to small-molecule quenchers.[59]

The third question raised by the discovery of the glycyl radical in pyruvate formate-lyase, how the radical is generated, is the subject of much of the remainder of this article. Work in the 1960s and 1970s demonstrated that pyruvate formate-lyase was activated under anaerobic conditions by an activating system that included an activating enzyme, *S*-adenosylmethionine, Fe(II), and reduced flavodoxin as a reductant.[60−62] Subsequent work showed that the activation of PFL involved the generation of a stable protein-centered radical, which was ultimately identified as a glycyl radical located on residue G734 of PFL.[23,32] Concomitant with generation of the glycyl radical, *S*-adenosylmethionine was cleaved to produce methionine and 5′-deoxyadenosine (Scheme 1). Label transfer studies demonstrated that a 5′ hydrogen atom of the 5′-deoxyadenosine product originated on the G734 residue of PFL, thereby suggesting that reductive cleavage of *S*-adenosylmethionine produces an intermediate 5′-deoxyadenosyl radical, which abstracts a hydrogen atom from G734 of PFL.[63] The H atom abstraction from G734 was shown to be stereospecific for the pro-S hydrogen.[63] A visible chromophore was observed in the purified activating enzyme, although it was not clear what was giving rise to the visible absorbance.[30] Work in the early 1990s further characterized the metal dependence of the pyruvate formate-lyase activating enzyme (PFL-AE), showing that Fe(II) stimulated activity and that other transition metals such as Cu(II) and Co(II) could not substitute for iron in the activation reaction.[64] In fact, some thiophilic transition metals, including Zn(II) and Cd(II), were shown to be effective inhibitors of the activation reaction, suggesting that the presumably mononuclear metal-binding site would involve cysteine ligands.[64]

Identification of an Iron−Sulfur Cluster in PFL-AE

Early work on PFL-AE was performed on enzyme purified under aerobic conditions[30] and, in some cases, on enzyme that had been completely denatured prior to purification and subsequently refolded.[64] Because PFL-AE is active in anaerobic bacteria and because it contained an as-yet unidentified metal center, we decided that, in order to identify the enzyme with its functionally relevant metal center, we would have to purify the protein without denaturation and without exposure to oxygen. Our early attempts to purify the protein in this manner involved simply using Ar-purged buffers on our protein purification columns and collecting protein fractions in a glovebag. This methodology allowed PFL-AE to be eluted from the column as a dark red-brown fraction; however, the color would rapidly fade if the fractions were not quickly frozen or transferred to more strictly anaerobic conditions. Once procedures were in place to isolate protein containing this chromophore, spectroscopic studies were initiated. UV−visible spectra revealed a chromophore with broad, overlapping transitions, characteristic

(54) Knappe, J.; Elbert, S.; Frey, M.; Wagner, A. F. V. *Biochem. Soc. Trans.* **1993**, *21*, 731−734.
(55) Sustmann, R.; Korth, H. G. *Adv. Phys. Org. Chem.* **1990**, *26*.
(56) Wong, K. K.; Kozarich, J. W. In *Metalloenzymes Involving Amino Acid-Residue and Related Radicals*; Sigel, H., Sigel, A., Eds.; Marcel Dekker: New York, 1994; Vol. 30, pp 361−404.
(57) Brocks, J. J.; Welle, F. M.; Beckhous, H.-D.; Rüchardt, C. *Tetrahedron Lett.* **1997**, *38*, 7721−7724.
(58) Himo, F. *Chem. Phys. Lett.* **2000**, *328*, 270−276.
(59) Becker, A.; Fritz-Wolf, K.; Kabsch, W.; Knappe, J.; Schultz, S.; Wagner, A. F. V. *Nature* **1999**, *6*, 969−975.
(60) Knappe, J.; Schacht, J.; Mockel, W.; Hopner, T.; Vetter, H. J.; Edenharder, R. *Eur. J. Biochem.* **1969**, *11*, 316−327.
(61) Knappe, J.; Blaschkowski, H. P. *Methods Enzymol.* **1975**, *41*.
(62) Knappe, J.; Schmitt, T. *Biochem. Biophys. Res. Commun.* **1976**, *71*, 1110−1117.
(63) Frey, M.; Rothe, M.; Wagner, A. F. V.; Knappe, J. *J. Biol. Chem.* **1994**, *269*, 12432−12437.
(64) Wong, K. K.; Murray, B. W.; Lewisch, S. A.; Baxter, M. K.; Ridky, T. W.; Ulissi-DeMario, L.; Kozarich, J. W. *Biochemistry* **1993**, *32*, 14102−14110.

Scheme 1. Reaction Catalyzed by Pyruvate Formate-Lyase Activating Enzyme

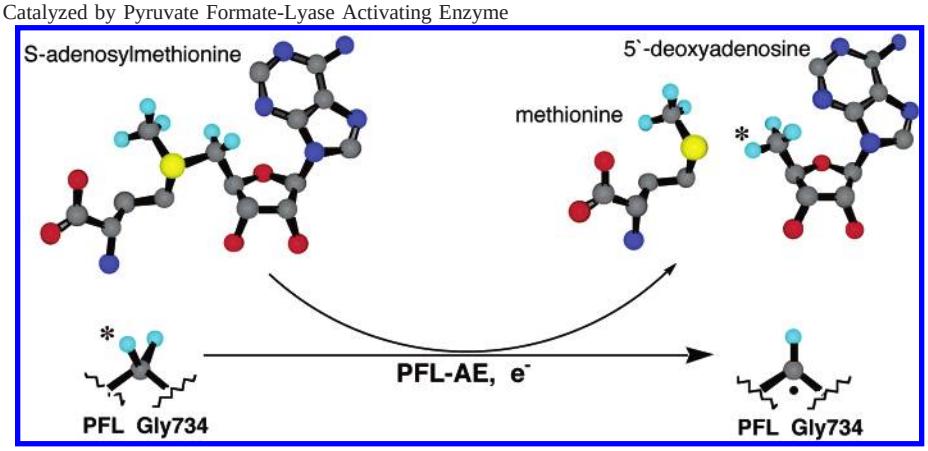

of an iron−sulfur cluster, although the type of cluster was not immediately obvious from the spectra. Iron and sulfide analyses confirmed this preliminary finding, as they showed approximately equivalent amounts of iron and sulfide in the protein. Using resonance Raman spectroscopy, we were able to further define the metal center as a mixture of $[2Fe-2S]^{2+}$ and $[4Fe-4S]^{2+}$ clusters in the isolated enzyme, with only $[4Fe-4S]^{2+}$ clusters remaining after reduction by dithionite.[35] EPR spectra of both of these states showed no signal, as expected for diamagnetic $[2Fe-2S]^{2+}$ and $[4Fe-4S]^{2+}$ clusters; however, if the protein was reduced in the presence of *S*-adenosylmethionine, a nearly axial signal ($g = 2.013, 1.889, 1.878$) characteristic of a $[4Fe-4S]^{+}$ cluster was observed.[35] These results suggested not only that *S*-adenosylmethionine affected the ability to reduce to the $[4Fe-4S]^{+}$ state, but that the $[4Fe-4S]^{+}$ state might be the catalytically active state, as it was the state present under reducing conditions in the presence of the cosubstrate *S*-adenosylmethionine.

Further modifications of our expression and purification conditions, which yielded more-soluble PFL-AE with a higher iron−sulfur cluster content, also slightly modified the cluster composition and behavior. EPR and resonance Raman spectroscopies now revealed the presence of a $[3Fe-4S]^{+}$ cluster ($g = 2.01, 1.94$) in the isolated enzyme that accounted for approximately two-thirds of the total iron in the sample.[37] The form of the remaining iron was identified using Mössbauer spectroscopy after the protein had been labeled with ^{57}Fe. Mössbauer spectra confirmed that approximately 67% of the iron was present in the form of a cuboidal $[3Fe-4S]^{+}$ cluster ($\delta = 0.28$ mm/s, $\Delta E_Q = 0.60$ mm/s), while the remaining 33% of the iron was found as a mixture of $[2Fe-2S]^{2+}$ ($\delta = 0.29$, $\Delta E_Q = 0.58$), $[4Fe-4S]^{2+}$ ($\delta = 0.45$, $\Delta E_Q = 1.15$), and linear $[3Fe-4S]^{+}$ clusters.[38] Addition of dithionite to this protein sample containing four different types of clusters resulted in a protein sample containing *only* $[4Fe-4S]^{2+/+}$ clusters.[38] This result was surprising both for the observation of numerous clusters and facile cluster interconversions, as outlined below, and for the ability to reduce to the $[4Fe-4S]^{+}$ state *in the absence of AdoMet*, which we had previously been unable to do (see above). It is not immediately obvious why our earlier and later preparations of PFL-AE, which differed only in the expression system used and in the degree to which anaerobic conditions were maintained during purification, differ in the ability to reduce to the $[4Fe-4S]^{+}$ in the absence of SAM.

It is unusual to find so many different clusters present in a single protein preparation, and this observation together with the ready conversion to [4Fe−4S] clusters suggested the presence of an unusually labile iron−sulfur cluster that could readily undergo transformations. Such cluster transformations are well-documented in synthetic model iron−sulfur chemistry;[1] however, it is fairly unusual to observe such transformations occurring cleanly in a biological system. One notable exception is aconitase, an enzyme of the citric acid cycle that uses a site-differentiated [4Fe−4S] cluster to bind substrate and catalyze dehydration/hydration reactions; in aconitase, the same four cluster types were observed, and the same transformation to [4Fe−4S] clusters occurred under reducing conditions.[65−67] In fact, aconitase and PFL-AE are the only two enzymes in which the unusual linear $[3Fe-4S]^{+}$ cluster has been observed.[38,67] At the time, we speculated as to whether the similar iron−sulfur cluster chemistries of aconitase and PFL-AE might be due to the presence of site-differentiated clusters in both enzymes.[38]

The reduced $[4Fe-4S]^{+}$ ($S = {}^1/_2$) cluster of PFL-AE was found to exhibit a rhombic EPR signal ($g = 2.02, 1.94, 1.88$).[48] This EPR signal was dramatically perturbed in the presence of SAM, affording a nearly axial signal ($g = 2.01, 1.88, 1.87$) (Figure 3).[48] The dramatic effect of SAM on the EPR signal of the $[4Fe-4S]^{+}$ cluster demonstrated a perturbation of the electronic environment of the cluster in the presence of SAM; this in turn suggested the intriguing possibility that SAM interacts directly with the [4Fe−4S] cluster of PFL-AE. Further exploration of interaction of SAM with the [4Fe−4S] cluster of PFL-AE is discussed in later sections.

Catalytic Activity of PFL-AE

Despite the unusual mixture of clusters present in purified PFL-AE, the enzyme was found to be catalytically active in

(65) Kent, T. A.; Dreyer, J. L.; Kennedy, M. C.; Huynh, B. H.; Emptage, M. H.; Beinert, H.; Münck, E. *Proc. Natl. Acad. Sci. U.S.A.* **1982**, *79*, 1096−1100.
(66) Kennedy, M. C.; Emptage, M. H.; Dreyer, J.-L.; Beinert, H. *J. Biol. Chem.* **1983**, *258*, 11098−11105.
(67) Kennedy, M. C.; Kent, T. A.; Emptage, M.; Merkle, H.; Beinert, H.; Münck, E. *J. Biol. Chem.* **1984**, *259*, 14463−14471.

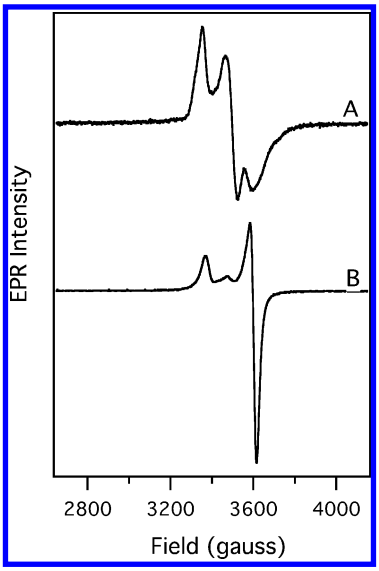

Figure 3. 9.5-GHz CW EPR spectra of PFL-AE photoreduced with deazariboflavin. (A) PFL-AE (0.7 mM) photoreduced for 1 h. The signal accounts for 197 μM $[4Fe-4S]^+$ based on EPR spin quantitation and has been multiplied by 3 for comparison purposes. (B) PFL-AE (0.78 mM) photoreduced for 1 h. followed by addition of 2 molar equiv of AdoMet. The signal accounts for 416 μM $[4Fe-4S]^+$ based on EPR spin quantitation. Conditions: T = 12 K, power = 20 μW, gain = 2.0×10^4, frequency = (A) 9.483 or (B) 9.476 GHz, modulation amplitude = (A) 8.231 or (B) 9.571 G. Reprinted from ref 48 with permission.

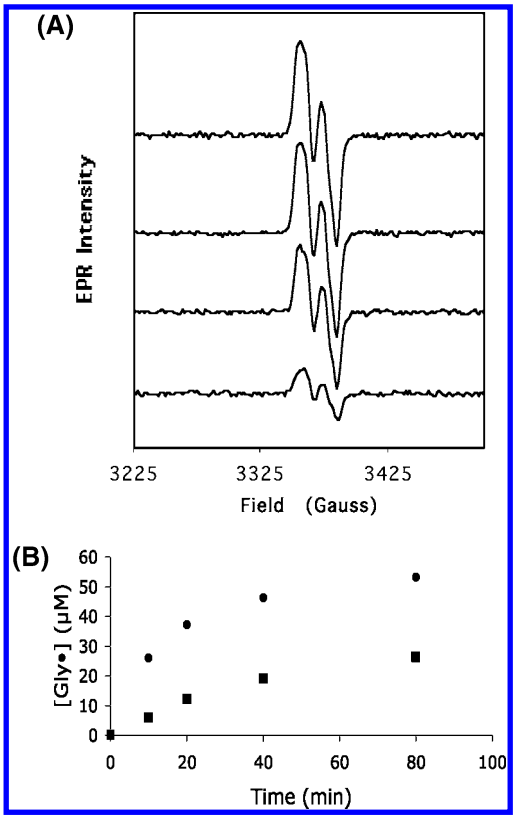

Figure 4. Assay of PFL-AE activity using EPR spectroscopy as described in Materials and Methods. (A) EPR spectra recorded at 10, 20, 40, and 80 min (bottom to top) during PFL activation. (B) Plots of the glycyl radical spin quantitation as a function of time for PFL-AE at 6.25 ug/mL (■) and 25 ug/mL (●); higher concentrations of AE provide a higher rate of activation, as expected. EPR parameters: T, 60 K; microwave power, 20 μW; microwave frequency, 9.48 GHz; modulation amplitude, 5.054 G.

the typical assay mixture, which includes PFL, PFL-AE, *S*-adenosylmethionine, and 5-deazariboflavin as a photoreductant.[35,37] The published assay for PFL-AE activity involves incubation of PFL-AE, PFL, *S*-adenosylmethionine, 5-deazariboflavin, and buffer components in the presence of an intense halogen lamp.[30,64,68] At varying time intervals, an aliquot of the mixture is removed and added to a cuvette containing pyruvate and CoA (the PFL substrates) as well as malic dehydrogenase, citrate synthase, and NAD, which are required for coupling PFL turnover to the spectroscopically detectable reduction of NAD^+ to NADH. PFL activity is thus measured indirectly via the coupling assay, and the amount of active PFL for that time point is then inferred, which allows for the calculation of the rate of PFL activation. All manipulations must be done under strict anaerobic conditions because of the extreme air sensitivity of the glycyl radical, and so, in addition to being an indirect assay of PFL-AE activity, it is quite cumbersome and prone to experimental error. Because of the difficulty of the published assay and our questions as to its reliability, we developed a simple and direct assay for PFL-AE activity that involves monitoring production of the PFL glycyl radical as a function of time by EPR spectroscopy (Figure 4). This assay provides a direct (although still discontinuous) measure of the rate of production of active PFL by PFL-AE. Using this assay method, we were able to obtain a specific activity for PFL-AE of 98000 pmol min^{-1} mg^{-1}, significantly higher than has been previously reported.[36,64] Removal of the cluster by oxidation and chelation of the iron, followed by gel filtration, resulted in complete loss of PFL-AE activity, demonstrating that the cluster was essential for the catalytic reaction.

Some comment is necessary here regarding the early reports of PFL-AE activity. Prior to discovery of the iron−sulfur cluster in PFL-AE, workers in other laboratories were able to observe the catalytic activity of PFL-AE. The earliest characterization of PFL-AE and its activity was done with enzyme purified in small quantities under aerobic conditions without denaturation.[30] Under these conditions, some of the iron−sulfur cluster present in the protein in vivo presumably survived the purification steps, as evidenced by the visible chromophore reported by these workers.[30] The observation that the addition of iron alone, in the absence of added sulfide, stimulated activity was presumably due to the presence of some excess sulfide, perhaps in the form of persulfides, in the purified protein, which, upon addition of iron, could contribute to the assembly of additional iron−sulfur clusters. Subsequent work done on PFL-AE that was completely denatured prior to purification and refolding reported a strict dependence of PFL-AE activity on the addition of Fe(II).[64] Again, no sulfide was added, as it was not known at the time that PFL-AE contained an iron−sulfur cluster, and yet activity was observed. In hindsight, it is likely that the presence of high concentrations of dithiothreitol (DTT) in the assay mixture provided a small amount of inorganic sulfide with which iron−sulfur clusters could be

(68) Brush, E. J.; Lipsett, K. A.; Kozarich, J. W. *Biochemistry* **1988**, *27*, 2217−2222.

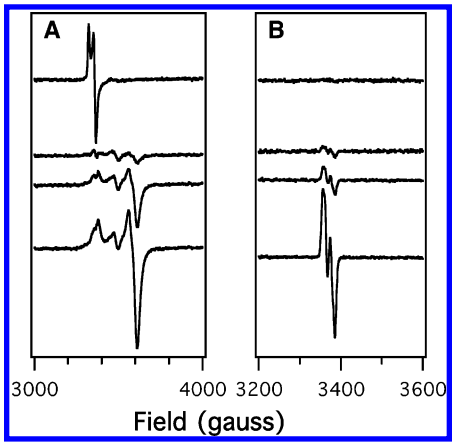

Figure 5. Correlation of the state of the iron−sulfur cluster on PFL-AE with the production of the glycyl radical on PFL. (A) PFL-AE in its as-isolated state was titrated with sodium dithionite (top to bottom, 0×, 1.25×, 1.5×, and 2.0× dithionite relative to protein concentration), and then a 10-fold excess of AdoMet was added, The gradual transformation of the $[3Fe-4S]^{+}$ cluster to a $[4Fe-4S]^{+}$ cluster upon reduction was monitored by EPR spectroscopy. (B) To each of the samples in A was added an equimolar amount of PFL, and EPR spectra were recorded to monitor production of the glycyl radical. The amount of glycyl radical produced on PFL correlated with the amount of reduced $[4Fe-4S]^{+}$ on PFL-AE. EPR parameters: *T*, (A) 12 or (B) 60 K; microwave power, (A) 2 mW or (B) 20 μW; microwave frequency, 9.48 GHz; modulation amplitude, (A) 10.084 or (B) 5.054 G.

assembled on PFL-AE upon addition of Fe(II). The relatively low specific activity of PFL-AE purified in this way (1300 pmol min^{-1} mg^{-1}) probably reflects the low efficiency of cluster reconstitution under these conditions.[64]

Identification of the Catalytically Active Cluster of PFL-AE

The studies described in the previous section clearly demonstrated, for the first time, the strict dependence of PFL-AE catalytic activity on the presence of the iron−sulfur cluster. Our observation of four different clusters in purified PFL-AE, however, raised an obvious question: Which cluster form was responsible for the catalytically required generation of the glycyl radical of PFL? Because reductant was required during the activation of PFL and because, in the presence of the reductant dithionite, only $[4Fe-4S]^{2+/+}$ clusters are observed in PFL-AE,[38] it was reasonable to propose that [4Fe−4S] clusters were involved in the catalytic activity of PFL-AE. However, direct evidence for the active cluster form was elusive, as reductant was required for PFL activation but reductant also caused cluster transformations.

The issue of the catalytically relevant cluster form was resolved through a series of quantitative EPR experiments performed under controlled reduction conditions. Initially, PFL-AE was titrated with dithionite, which resulted in a gradual conversion of the "as-isolated" protein (containing primarily $[3Fe-4S]^{+}$ clusters) to reduced protein containing a significant quantity of $[4Fe-4S]^{+}$ clusters, as observed by EPR spectroscopy after addition of SAM (Figure 5A). Aliquots of the PFL-AE/SAM mixture were taken at each titration step; to these aliquots were added equimolar amounts of PFL, and then EPR spectra were recorded at 60 K to monitor production of the PFL glycyl radical without interference from the iron−sulfur cluster signals, which are

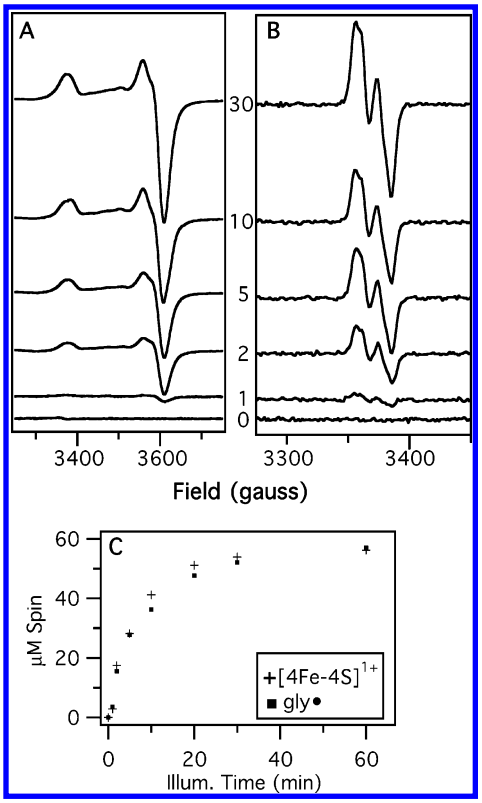

Figure 6. EPR-detected single-turnover experiments to define the catalytically active iron−sulfur cluster in PFL-AE. (A) EPR spectra of samples containing PFL-AE, SAM, and 5-deazariboflavin as a function of illumination (reduction) time in minutes. (B) EPR spectra of samples as in A to which PFL has been added prior to freezing for EPR. (C) EPR spin quantitation of the $[4Fe-4S]^{+}$ and glycyl radical signals shows a 1:1 correspondence. Reprinted from ref 46 with permission.

unobservable at 60 K (Figure 5B). It was clear from these experiments that the amount of glycyl radical produced correlated with the state of reduction of the PFL-AE iron−sulfur cluster.

To examine this issue more clearly, we used 5-deazariboflavin-mediated photoreduction of PFL-AE to achieve single-turnover conditions.[46] The advantage of photoreduction is that it can be used to reduce the PFL-AE iron−sulfur cluster to a specified state, and then excess reductant can be easily removed by simply placing samples in the dark. This then allows monitoring of the reactivity of specific cluster states of PFL-AE, without interference from reductants that might cause cluster interconversions. Furthermore, changes in cluster state due to enzymatic turnover could be monitored. The results of these experiments are shown in Figure 6.[46] The starting state for the protein prior to photoreduction is the diamagnetic $[4Fe-4S]^{2+}$ state in these experiments, and with increasing time of photoreduction, increasing amounts of $[4Fe-4S]^{+}$ cluster (g = 2.01, 1.89, 1.88) are observed by EPR spectroscopy, as seen in Figure 6, panel A. These EPR spectra of PFL-AE are recorded in the presence of *S*-adenosylmethionine, which is *not* reductively cleaved by PFL-AE in the absence of PFL. At each time point of photoreduction, the PFL-AE + *S*-adenosylmethionine sample was divided: half of the sample was used directly for EPR analysis, and the other half was mixed with an equimolar amount of PFL before being frozen for EPR analysis. EPR

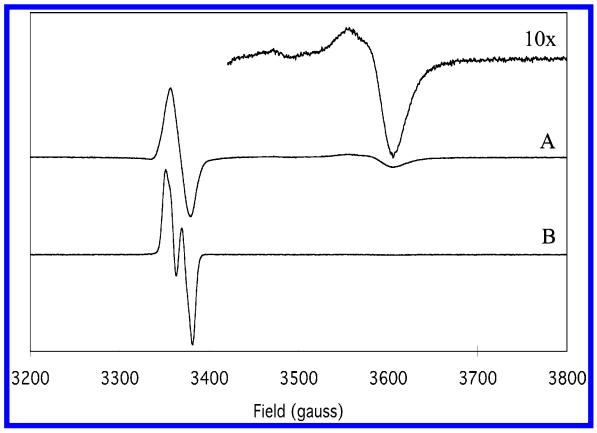

Figure 7. Regeneration of the PFL-AE $[4Fe-4S]^{+}$ signal upon re-illumination of the single-turnover samples in Figure 5. Samples from Figure 5B were re-illuminated, resulting in simultaneous presence of both the $[4Fe-4S]^{+}$ on PFL-AE and the glycyl radical on PFL. EPR parameters: *T*, 12 K; microwave power, (A) 1.99 mW or (B) 1.99 μW; microwave frequency, 9.47 GHz; modulation amplitude, 5.054 G.

spectra of the samples containing PFL are shown in Figure 6, panel B. It is clear from these spectra that the $[4Fe-4S]^{2+}$ state of PFL-AE is unable to generate the glycyl radical on PFL in the absence of exogenous reductant; however, as the amount of $[4Fe-4S]^{+}$ cluster on PFL-AE increases, the amount of glycyl radical produced on PFL also increases. EPR spin quantitation reveals a 1:1 correspondence between the amount of $[4Fe-4S]^{+}$ on PFL-AE and the amount of glycyl radical generated on PFL (Figure 6, panel C).[46] Also apparent from these spectra is the disappearance of the $[4Fe-4S]^{+}$ EPR signal concomitant with appearance of the glycyl radical EPR signal (the glycyl radical EPR spectra shown were recorded at 60 K, a temperature at which the $[4Fe-4S]^{+}$ signal is not observed; however, when recorded at 12 K, the samples included in panel B of Figure 6 showed no evidence for a $[4Fe-4S]^{+}$ EPR signal). Taken together, these results provide strong evidence that the $[4Fe-4S]^{+}$ state of PFL-AE is the catalytically active state and that this reduced cluster provides the electron necessary for reductive cleavage of *S*-adenosylmethionine and subsequent abstraction of a H atom from G734 of PFL as shown in Scheme 1. Thus, one $[4Fe-4S]^{+}-$PFL-AE generates one PFL-Gly$^{\bullet}$ and, in the process, is oxidized to $[4Fe-4S]^{2+}-$PFL-AE.[46]

To further investigate this process, the samples to which PFL had been added (Figure 6, panel B) were re-illuminated to see whether the $[4Fe-4S]^{+}-$PFL-AE could be regenerated Figure 7). The resulting EPR spectra clearly show the presence of *both* the PFL glycyl radical and the PFL-AE-reduced $[4Fe-4S]^{+}$ cluster. The two EPR-active species are now observed simultaneously because there is only a 1:1 molar ratio of PFL to PFL-AE; with no additional PFL to activate, the PFL-AE remains in the reduced state upon photoreduction. Together, these EPR studies provide evidence for a mechanism in which PFL-AE cycles between the $[4Fe-4S]^{+}$ and $[4Fe-4S]^{2+}$ states during catalysis. This mechanism suggests the possibility that the [4Fe−4S] cluster of PFL-AE is a simple electron-transfer cluster, not unlike the many other iron−sulfur clusters involved in electron-transfer reactions in biology. However, we have estimated the redox potential of PFL-AE to be on the order of −500 mV (data not shown), whereas sulfonium centers similar to SAM generally have redox potentials significantly more negative than −1 V;[69] this large mismatch in redox potential argues against a "simple" long-range electron-transfer process to initiate the PFL-AE catalyzed reaction. The analogy to B_{12} mentioned above, together with the information provided in the following section, led us to favor mechanistic possibilities involving a direct interaction between the iron−sulfur cluster and *S*-adenosylmethionine.

Iron−Sulfur Clusters and the Cluster-Binding Motif in the Radical-SAM Superfamily

All of the radical-SAM enzymes characterized to date contain iron−sulfur clusters, although the detailed properties of the clusters vary from enzyme to enzyme. As outlined above, PFL-AE was isolated with a $[3Fe-4S]^{+}$ cluster as its primary cluster form,[37,38] and this cluster is converted to the $[4Fe-4S]^{2+/+}$ cluster upon reduction. Lysine 2,3-aminomutase exhibits similar (though not identical) cluster chemistry, with intact $[4Fe-4S]^{2+/3+}$ clusters present in the isolated protein and $[3Fe-4S]^{+}$ clusters observed upon oxidation.[39] Biotin synthase, however, contains $[2Fe-2S]^{2+}$ clusters in the isolated protein and $[4Fe-4S]^{2+}$ clusters upon reduction[70,71] and has not been shown to contain $[3Fe-4S]^{+}$ clusters under any conditions. More recently, it has been found that, under appropriate reconstitution conditions, biotin synthase contains *both* $[2Fe-2S]^{2+}$ and $[4Fe-4S]^{2+}$ clusters.[72−75] Likewise, only [2Fe−2S] and [4Fe−4S] clusters have been observed in lipoate synthase,[76−78] and only [4Fe−4S] clusters have been identified in HemN.[50] Therefore, although the details of cluster chemistry vary from enzyme to enzyme in this superfamily, a recurring theme is the presence of a [4Fe−4S] cluster in the radical-SAM enzymes under certain conditions; the observation of the [4Fe−4S] cluster throughout the superfamily is consistent with the results reported above demonstrating the catalytic relevance of this cluster for PFL-AE.[46]

Coordination of [4Fe−4S] clusters in proteins is generally via four cysteine side chains, and frequently, these cysteines are arranged in a specific and recognizable cluster-binding motif in the amino acid sequence of the protein. One of the

(69) Grimshaw, J. In *Chemistry of the Sulphonium Group*; Stirling, C. J. M., Ed.; Wiley: Chichester, U.K., 1981; pp 141−155.
(70) Duin, E. C.; Lafferty, M. E.; Crouse, B. R.; Allen, R. M.; Sanyal, I.; Flint, D. H.; Johnson, M. K. *Biochemistry* **1997**, *36*, 11811−11820.
(71) Tse Sum Bui, B.; Florentin, D.; Marquet, A.; Benda, R.; Trautwein, A. X. *FEBS Lett.* **1999**, *459*, 411−414.
(72) Ugulava, N. B.; Gibney, B. R.; Jarrett, J. T. *Biochemistry* **2001**, *40*, 8343−8351.
(73) Ugulava, N. B.; Sacanell, C. J.; Jarrett, J. T. *Biochemistry* **2001**, *40*, 8352−8358.
(74) Ugulava, N. B.; Surerus, K. K.; Jarrett, J. T. *J. Am. Chem. Soc.* **2002**, *124*, 9050−9051.
(75) Tse Sum Bui, B.; Benda, R.; Schünemann, V.; Florentin, D.; Trautwein, A. X.; Marquet, A. *Biochemistry* **2003**, *42*, 8791−8798.
(76) Busby, R. W.; Schelvis, J. P. M.; Yu, D. S.; Babcock, G. T.; Marletta, M. A. *J. Am. Chem. Soc.* **1999**, *121*, 4706−4707.
(77) Ollagnier-de Choudens, S.; Fontecave, M. *FEBS Lett.* **1999**, *453*, 25−28.
(78) Cicchillo, R. M.; Lee, K.-H.; Baleanu-Gogonea, C.; Nesbitt, N. M.; Krebs, C.; Booker, S. J. *Biochemistry* **2004**, *43*, 11770−11781.

Scheme 2. Incorporation of ^{57}Fe into the Unique Iron Site of the [4Fe−4S] Cluster of PFL-AE

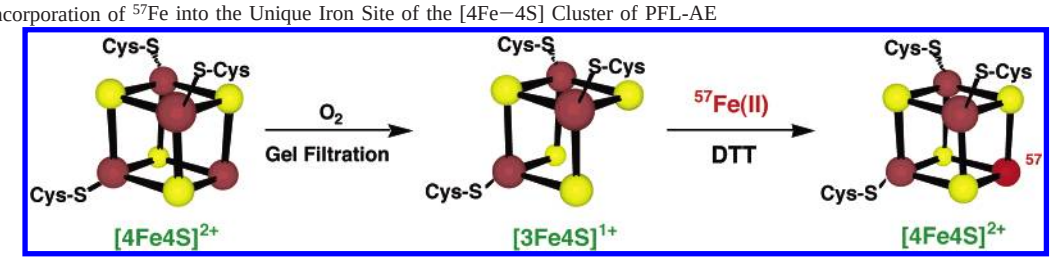

characteristic features of members of the radical-SAM superfamily is a three-cysteine motif (CX_3CX_2C),[20] which, except for the presence of three (rather than four) cysteines in the motif, is reminiscent of cluster-binding motifs in other iron−sulfur proteins. The cysteines in this CX_3CX_2C motif appear to provide the protein ligands for the [4Fe−4S] cluster in these enzymes, based on site-directed mutagenesis studies[36,78,79] and, more recently, X-ray crystal structures[50−52] of several members of the radical-SAM superfamily. The conservation of the three-cysteine motif throughout the radical-SAM superfamily, together with the evidence that these three cysteines alone are important in cluster coordination, implies that a *site-differentiated iron−sulfur cluster*, in which one of the four irons is coordinated by a noncysteinal ligand, is a significant structural feature of the radical-SAM enzymes.

Identification of a Unique Iron Site in PFL-AE

As discussed above, purified PFL-AE contained primarily $[3Fe−4S]^+$ cluster which could be converted to the catalytically relevant [4Fe−4S] cluster by reduction. The $[3Fe−4S]^+$ cluster is an all-ferric cluster and is generally a product of oxidative degradation of a [4Fe−4S] cluster. In fact we found that exposing [4Fe−4S]−PFL-AE to oxidants such as O_2 or ferricyanide results in conversion to primarily $[3Fe−4S]^+$ clusters. We attributed this behavior to the predicted presence of a site-differentiated [4Fe−4S] cluster with one iron coordinated by a noncysteinal ligand, which would presumably make that iron more labile than the other three irons in the cluster. Although not all of the other characterized radical-SAM enzymes show a propensity for formation of $[3Fe−4S]^+$ clusters, all have the conserved three-cysteine motif, which strongly implies a functional significance for a site-differentiated [4Fe−4S] cluster.

We utilized this apparent enhanced lability of one iron of the [4Fe−4S] cluster to achieve site-specific labeling of the unique site with ^{57}Fe (Scheme 2).[80] After the [4Fe−4S]−PFL-AE had been exposed to oxidant, the released iron was removed by gel filtration chromatography and the $[3Fe−4S]^+$ formed was quantified by EPR spectroscopy. An equimolar equivalent of ^{57}Fe(II) and a small excess of dithiothreitol (DTT) was then added, and the resulting protein, which was EPR-silent, was examined by Mössbauer spectroscopy in the absence and presence of *S*-adenosylmethionine (Figure 8).[80] The results show that the added ^{57}Fe(II) is incorporated into the cluster, as spectrum A is a typical quadrupole doublet for iron in a $[4Fe−4S]^{2+}$ cluster (δ = 0.42 mm/s, ΔE_Q = 1.12 mm/s). The Mössbauer spectrum is dramatically perturbed, however, upon addition of SAM, as shown by spectrum B and the difference spectrum C in Figure 8. A new quadrupole doublet appears with parameters (δ = 0.72 mm/s, ΔE_Q = 1.15 mm/s) that are inconsistent with the typical iron environment in a $[4Fe−4S]^{2+}$ cluster and suggest an increase in coordination number and/or binding of more ionic ligands to the unique site iron.[80] Significantly, when a $[3^{57}Fe−4S]^+$ cluster is generated in ^{57}Fe-enriched PFL-AE and natural-abundance Fe(II) and DTT are added, no perturbation of the Mössbauer spectrum is observed upon addition of SAM, consistent with the selective binding of the added iron to the unique site.[80] Taken together, these results clearly demonstrated for the first time the presence of a unique iron site in the [4Fe−4S] cluster of PFL-AE and provided evidence for interaction of SAM with the unique iron site.

Coordination of *S*-Adenosylmethionine to the Unique Iron Site

Interaction with the Catalytically Essential Reduced State. The catalytically essential $[4Fe−4S]^+$ ($S = {}^1/_2$) cluster

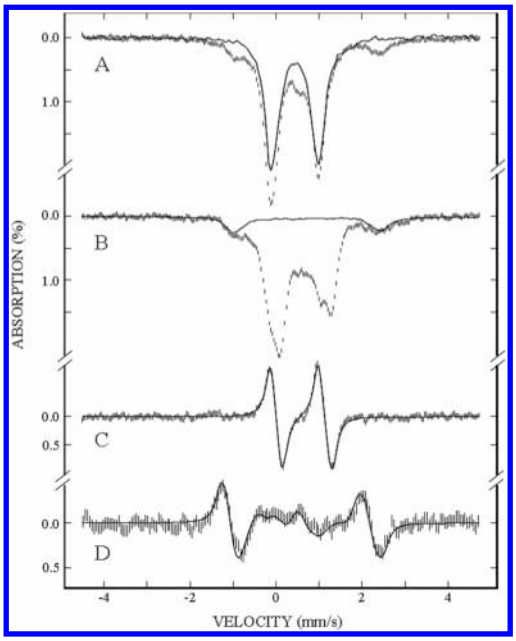

Figure 8. Mössbauer spectra of PFL-AE site-specifically labeled at the unique iron site with ^{57}Fe. (A) $3^{56}Fe1^{57}Fe4S]^{2+}$−PFL-AE in the absence of SAM. (B) $[3^{56}Fe1^{57}Fe4S]^{2+}$−PFL-AE in the presence of SAM. (C) Difference spectrum B − A. (D) Difference spectrum of spectra recorded at high field. Reprinted from ref 80 with permission.

(79) Tamarit, J.; Gerez, C.; Meier, C.; Mulliez, E.; Trautwein, A.; Fontecave, M. *J. Biol. Chem.* **2000**, *275*, 15669−15675.
(80) Krebs, C.; Broderick, W. E.; Henshaw, T. F.; Broderick, J. B.; Huynh, B. H. *J. Am. Chem. Soc.* **2002**, *124*, 912−913.

of PFL-AE is EPR-active, as shown above, and this allowed us to use electron−nuclear double resonance (ENDOR) spectroscopy to define the interaction of SAM with the [4Fe−4S] cluster of PFL-AE, which, in turn, provides important insights into the mechanism of radical generation.[48,49] To investigate the possibility of coordination of SAM to the unique site of the [4Fe−4S] cluster of PFL-AE, we prepared isotopically labeled *S*-adenosylmethionine in order to probe the coupling between the paramagnetic iron−sulfur cluster and specific nuclei on SAM. The amino and carboxylate moieties of SAM were the most likely candidates for coordination to the unique iron site, so SAM was synthesized with ^{17}O at the carboxylate oxygen, with ^{13}C at the carboxylate carbon, and with ^{15}N at the amine nitrogen.[49] Each labeled SAM was added to photoreduced $[4Fe-4S]^{+}$−PFL-AE, and the solutions were frozen for ENDOR measurements. The observation of ENDOR signals for all three nuclei (Figure 9) demonstrated for the first time that SAM forms a classical five-membered chelate ring with the unique iron of the [4Fe−4S] cluster of PFL-AE (Chart 1).[49] The ^{17}O (12.2 MHz) and ^{13}C (0.71 MHz) couplings observed in the PFL-AE/SAM complex are very similar to those found for aconitase with carboxylate-labeled citrate/isocitrate.[81,82] The strong couplings support direct coordination of a carboxylate oxygen of SAM to the unique iron in PFL-AE, as was also seen in the aconitase enzyme−substrate complex. The ^{15}N coupling (5.8 MHz) is comparable to those observed for ^{15}N ligands in other enzyme systems (^{15}N-histidine bound to the Rieske [2Fe−2S] cluster[83] and ^{15}N-ACC (ACC = 1-aminocyclopropane-1-carboxylic acid) coordinated to the non-heme iron of ACC oxidase[84]) and again is consistent with direct coordination.

Field-Dependence of the ^{13}C, ^{17}O, and ^{15}N ENDOR Data. 2D field-frequency plots of ENDOR spectra collected across the EPR envelope were obtained from photoreduced $[4Fe-4S]^{+}$−PFL-AE in the presence of (i) carboxyl-^{13}C−SAM (ii) carboxyl-^{17}O−SAM, and (iii) amino-^{15}N−SAM. Simulation of the 2D patterns allowed determination of the details of the coordination of the methionine fragment of SAM to the unique iron of the [4Fe−4S] cluster. We reported previously that large ^{17}O and ^{15}N couplings observed in the presence of (ii) and (iii) indicate direct coordination of SAM to the unique iron via a five-membered-ring chelate.[49] Analysis of the field dependence of these interactions as well as the carboxyl-^{13}C interaction allows a full analysis of the geometry and bonding of SAM to the 4Fe−4S cluster.

(i) Carboxyl-^{13}C−SAM. Figure 10 presents the 2-D Mims pulsed ^{13}C ENDOR patterns for $[4Fe-4S]^{+}$−PFL-AE (reduced photolytically) with carboxyl-^{13}C−SAM. The signal intensities have been normalized to the height of the electron

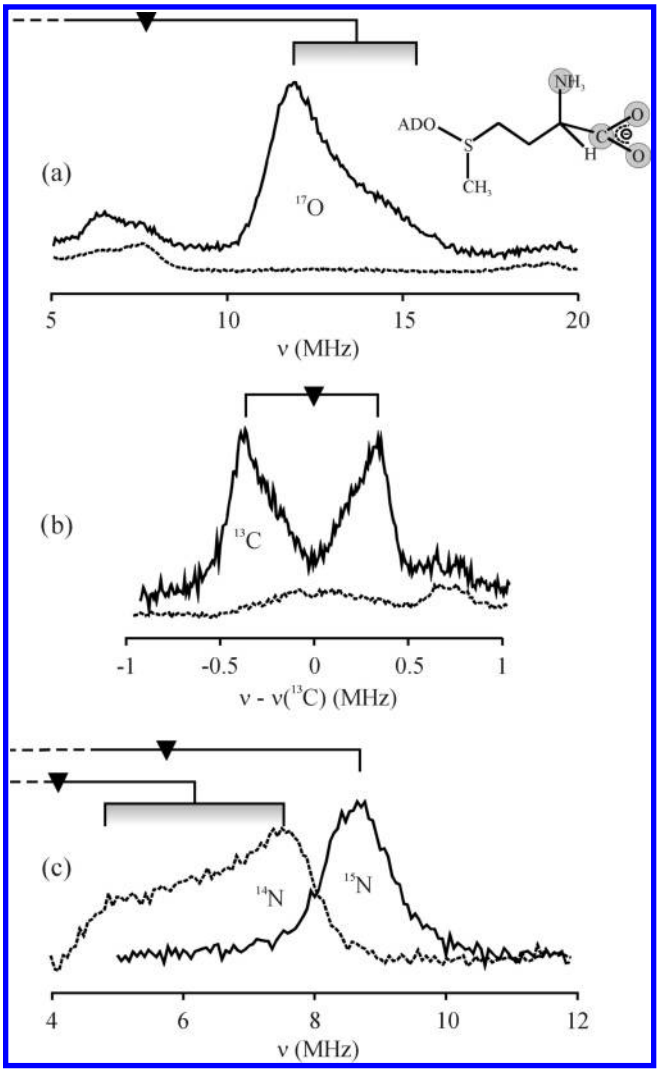

Figure 9. 35-GHz pulsed ENDOR spectra of PFL-AE wit (a) h ^{17}O and (b) ^{13}C carboxylato-labeled and (c) ^{15}N-amino-labeled AdoMet compared with data from an unlabeled sample, at $g_{\perp}$ Conditions: $T = 2$ K. (a) ^{17}O-labeled, Davies ENDOR. $\nu_{MW} = 34.9$ MHz; microwave pulse lengths = 80, 40, 80 ns; RF pulse length = 60 ms. Number of averaged transients at each point: ^{17}O, 288; unlabeled, 200. (b) ^{13}C-labeled, Mims ENDOR. $\nu_{MW} = 34.8$ MHz, microwave pulse lengths = 80 ns, $\tau = 552$ ns, RF pulse length = 60 ms. Number of averaged transients: ^{13}C-labeled, 144; unlabeled, 600. (c) ^{15}N-labeled, Davies ENDOR. $\nu_{MW} = 34.9$ MHz; microwave pulse lengths = 80, 40, 80 ns; RF pulse length = 60 ms. Number of average transients: ^{15}N-labeled, 80; unlabeled, 624. Reprinted from ref 49 with permission.

spin−echo to enable analysis of the effect of signal suppression from the Mims pulse sequence used in these experiments. As explained in Materials and Methods and discussed extensively elsewhere,[48] although Mims pulsed ENDOR spectroscopy is the best method for measuring small couplings, there is a suppression "hole" with zero ENDOR intensity at the Larmor frequency (in this case, $\Delta\nu(^{13}C) = 0$ MHz), corresponding to $A = 0$. This masks the difference between isotropic hyperfine interactions, which do not produce spectral intensity near $A = 0$, and dipolar interactions, which do so for certain orientations. The isotropic interaction and local contributions to the anisotropic interaction are useful for determining bonding and delocalization, while the nonlocal dipolar interactions between an electron spin and a nucleus not involved in spin delocalization can

(81) Kennedy, M. C.; Werst, M.; Telser, J.; Emptage, M. H.; Beinert, H.; Hoffman, B. M. *Proc. Natl. Acad. Sci. U.S.A.* **1987**, *84*, 8854−8858.
(82) Werst, M. M.; Kennedy, M. C.; Beinert, H.; Hoffman, B. M. *Biochemistry* **1990**, *29*, 10526−10532.
(83) Gurbiel, R. J.; Doan, P. E.; Gassner, G. T.; Macke, T. J.; Case, D. A.; Ohnishi, T.; Fee, J. A.; Ballou, D. P.; Hoffman, B. M. *Biochemistry* **1996**, *35*, 7834−3845.
(84) Rocklin, A. M.; Tierney, D. L.; Kofman, V.; Brunhuber, N. M. W.; Hoffman, B. M.; Christoffersen, R. E.; Reich, N. O.; Lipscomb, J. D.; Que, L., Jr. *Proc. Natl. Acad. Sci. U.S.A.* **1999**, *96*, 7905−7909.

Chart 1. Interaction of *S*-adenosylmethionine with the [4Fe−4S] Cluster of PFL-AE and Position of Isotopic Labels Used for ENDOR Spectroscopy

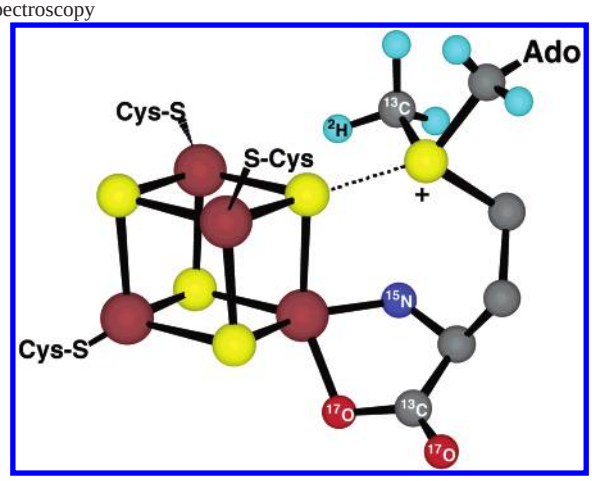

be used to determine the electron−nuclear distance and the orientation of the nucleus within the *g*-tensor coordinate frame. Using a procedure similar to that applied in the analysis of the ^{13}C ENDOR spectra from [4Fe−4S]$^{+}$−PFL-AE with $^{13}CH_3$−SAM,[48] we simulated both the spectral shapes *and* the intensities to obtain the ^{13}C hyperfine tensor: $\mathbf{A}(^{13}C) = [-1.1, 0.95, 0.82]$ MHz and Euler angles, relative to the *g*-tensor frame, of $\theta = 30°$ and $\varphi = 0°$. The ^{13}C tensor can be decomposed into the sum of an isotropic component, $a_{iso}(^{13}C) = 0.22$ MHz, and two mutually perpendicular dipolar tensors, $\mathbf{T}(^{13}C) = [-2T, T, T] = [-1.28, 0.64, 0.64]$ MHz and $\mathbf{t}(^{13}C) = [t, -2t, t] = [-0.04, 0.09, -0.04]$ MHz. The first of these is assigned to the through-space dipolar interaction between the cluster spin and the ^{13}C nucleus. The latter is derived from a local interaction with electron spin density on the carbon atom itself with the ^{13}C nucleus. This anisotropic term is correlated with the isotropic coupling as the spin on carbon is in an sp^n hybrid, with the p-orbital contribution giving the former

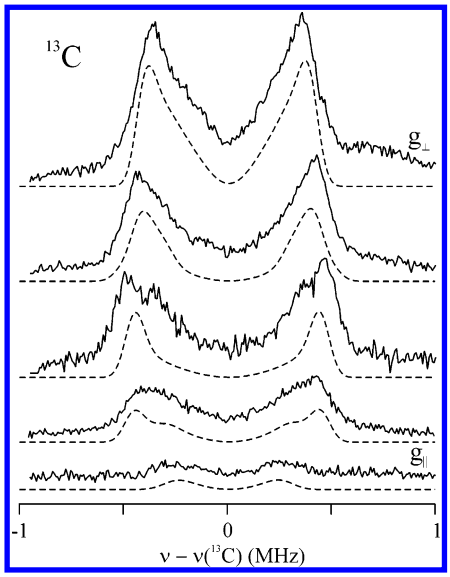

Figure 10. Field dependence data (—) and simulations (− − −) from 35-GHz Mims pulsed ENDOR of PFL-AE with carboxy-^{13}C−SAM, with conditions as in Figure 9. Simulation parameters: $\mathbf{A} = [1.1, -0.95, -0.82]$, $\alpha = 30$, $\beta = \gamma = 90$, EPR line width = 120 MHz, ENDOR line width = 0.1 MHz, $\tau = 562$ ns. Mims suppression effects are included.

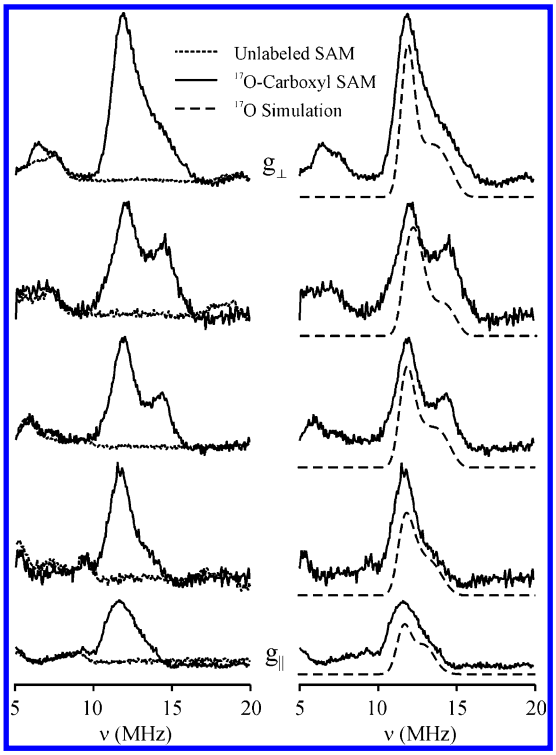

Figure 11. 35-GHz Davies ENDOR spectra of PFL-AE^{+} with unlabeled SAM and with ^{17}O-carboxyl SAM. Left: Comparison of ENDOR from ^{17}O-labeled and unlabeled SAM. Right: ^{17}O ENDOR and simulations. Experimental conditions: $T = 2$ K; Davies pulse sequence; microwave pulse lengths = 80, 40, 80 ns; repetition rate = 100 Hz; RF pulse length = 60 ms. ^{17}O Simulation parameters: Program GENDOR, $\mathbf{A} = [8.6, 14.4, 8.2]$, $\alpha = 30$, $\beta = \gamma = 0$, $\mathbf{P} = [-0.05. 0.1, -0.05]$, $\alpha = 30$, $\beta = \gamma = 0$, ENDOR line width = 0.5 MHz, EPR line width = 100 MHz.

and the s-orbital contribution the latter. From $\mathbf{T}(^{13}C)$, we can approximate r(Fe(unique)−^{13}C) by neglecting any interaction with spins on other atoms of the cluster, assuming a point-dipole−point-dipole interaction, and taking $n = 3$, which gives

$$T = g\beta g_N \beta_N K(3/4)/r(\mathrm{Fe}-^{13}\mathrm{C})^3 \qquad (1)$$

where the constant terms have their usual meaning and K is the spin projection coefficient for the unique Fe of the spin-coupled $S = {}^1/_2$ cluster. Although the values of K for PFL-AE are not known, it is reasonable to use the known coefficients of substrate-bound aconitase (ES), which also has a labile, noncysteine cluster ligand: $K = 1.57$. This gives (Fe(unique)−^{13}C) = 3.3 ± 0.1 Å.

There is as yet no crystal structure of PFL-AE, but there are reports of crystal structures from three other members of the radical-SAM superfamily. These are (i) coproporphyrinogen III oxidase (HemN),[50] (ii) biotin synthase (BioB),[51] (iii) the ligand binding protein MoaA.[52] Comparison of the structures of these three proteins reveals that the geometry of SAM binding is similar in each case. The distance from the unique Fe to the carboxyl carbon of bound SAM is in the range of 2.92−3.15 Å. Considering the crudeness of the ENDOR estimate, it is in quite satisfactory agreement.

(ii) Carboxyl-^{17}O−SAM, (iii) Amino-^{15}N−SAM. Figures 11 and 12 present 2D field-frequency ENDOR patterns for these two nuclei, along with simulations of these patterns

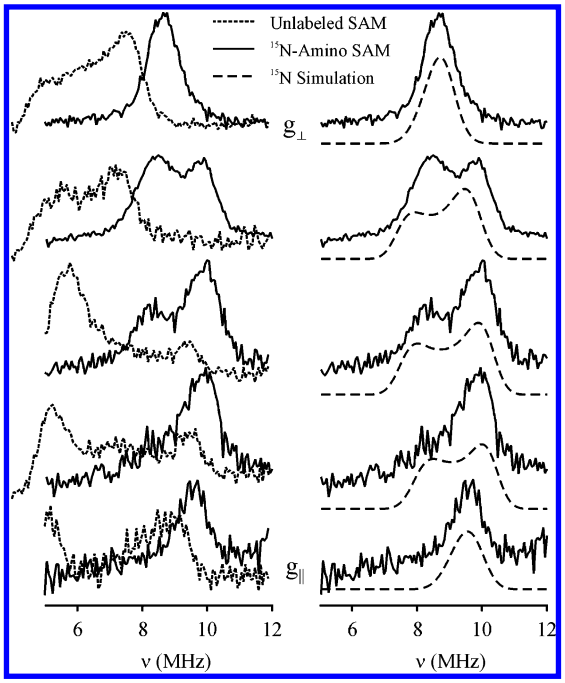

Figure 12. 35-GHz Davies ENDOR of PFL-AE$^+$ with unlabeled SAM and with ^{15}N-amino SAM. Left: Comparison of ^{14}N and ^{15}N ENDOR. Right: ^{15}N ENDOR and simulations. Experimental conditions: $T = 2$ K; Davies pulse sequence; microwave pulse lengths = 80, 40, 80 ns; repetition rate = 100 Hz; RF pulse length = 60 ms. ^{15}N Simulation parameters: Program ENDORSIM, $\mathbf{A} = [9.7, 6, 3.5]$, $\alpha = 0$, $\beta = 30$, $\gamma = 0$, ENDOR line width = 0.8 MHz, EPR line width = 300 MHz.

calculated with programs ENDORSIM for ^{15}N[85] and GENDOR for ^{17}O.[86] As shown, the patterns are well reproduced by simulations that use tensors with significant isotropic components ($a_{iso}(^{15}N) = 6.4$ MHz, $a_{iso}(^{17}O) = 10.7$ MHz), as expected for direct coordination to an Fe of the reduced Fe−S cluster. Taking into account the couplings expected for unit spin in the 2s orbitals of a ^{15}N and ^{13}C, these correspond to comparable low spin densities, ∼ 1% for sp^3 orbitals. However, the ^{15}N dipolar tensor is highly rhombic, whereas the dipolar component of the hyperfine interaction with ^{17}O is nearly axial, an indication of the expected difference in hybridization of the two atoms.

Interaction of the Sulfonium of SAM with the [4Fe−4S] Cluster

Coordination of the methionine portion of SAM to the unique iron of the [4Fe−4S] cluster of PFL-AE is intriguing, as it suggests that the unique iron serves as an anchor to hold the cosubstrate SAM in place for reaction. The business end of SAM, however, is the sulfonium, as it is the S−C(5′) bond that is reductively cleaved in catalysis, and so there was considerable interest in investigating the proximity of this moiety to the cluster. ENDOR spectroscopy of [4Fe−4S]$^+$−PFL-AE in the presence of methyl-^{2}H−SAM and methyl-^{13}C−SAM addressed this question (Figure 13).[48] The ^{2}H ENDOR spectra revealed a substantial ^{2}H coupling of ∼1 MHz (corresponding to a ^{1}H coupling of 6−7 MHz), requiring that the methyl deuterons be in close proximity to the [4Fe−4S]$^+$ cluster (estimated as 3.0−3.8 Å to the nearest iron of the cluster). The methyl-^{13}C coupling to the [4Fe−4S]$^+$ cluster was found to comprise both "nonlocal" dipolar interactions and a "local" term arising from spin density on the ^{13}C. The presence of spin density at the methyl-^{13}C requires not only that SAM lies close to the [4Fe−4S]$^+$ cluster, but that there be some local orbital overlap with the cluster, as orbital overlap would be required to delocalize spin density from the [4Fe−4S]$^+$ cluster onto the methyl-^{13}C of SAM. We proposed that this orbital overlap occurred via interaction of one of the μ_3-bridging sulfides of the [4Fe−4S]$^+$ cluster with the sulfonium of SAM (Chart 1).[48] The spectroscopic results, taken together, provided a working model for SAM binding in which the methionine portion of SAM serves to anchor the cosubstrate in place by coordination to the unique site of the cluster such that the sulfonium sulfur is in close contact with one of the μ_3-bridging sulfides of the cluster; this close contact is proposed to provide the pathway for inner-sphere electron transfer from the cluster to SAM to initiate the radical reaction.[48,49]

Interaction with the [4Fe−4S]$^{2+}$ State. ENDOR spectroscopy of the reduced [4Fe−4S]$^+$ state of PFL-AE in the presence of labeled SAMs provided the first evidence for the direct interaction of SAM with the catalytically active state of a radical-SAM enzyme. However, an equally important question is whether and how SAM interacts with the oxidized [4Fe−4S]$^{2+}$ state, as evidence suggests this is a prominent state in the catalytic cycle.[46] The [4Fe−4S]$^{2+}$ state cannot be probed directly by ENDOR spectroscopy because it is diamagnetic. We therefore used a cryoreduction technique[87−93] to generate the [4Fe−4S]$^+$ state of PFL-AE trapped in the geometry of the [4Fe−4S]$^{2+}$ state. The technique involves adding labeled SAM to the [4Fe−4S]$^{2+}$ state of the enzyme and then freezing the sample in liquid nitrogen. Then, at 77 K, the sample is γ-irradiated, producing electrons that reduce a fraction of the iron−sulfur clusters to the 1+ state while the clusters are trapped in the 2+ state geometry. The reduced clusters prepared in this way, referred to as [4Fe−4S]$^{2+}_{RED}$, can then be probed by ENDOR spectroscopy to examine the interaction between SAM and the cluster in the [4Fe−4S]$^{2+}$ state.

ENDOR spectra of [4Fe−4S]$^{2+}_{RED}$−PFL-AE in the presence of methyl-^{2}H−SAM and methyl-^{13}C−SAM are essentially identical to spectra obtained on samples of [4Fe−4S]$^+$−PFL-AE in the presence of the same labeled substrates (Figure 13), demonstrating that the sulfonium−SAM interac-

(85) Doan, P. E., 2003.
(86) Hoffman, B. M.; DeRose, V. J.; Doan, P. E.; Gurbiel, R. J.; Houseman, A. L. P.; Telser, J. In *Biological Magnetic Resonance*; Berliner, L. J., Reuben, J., Eds.; Plenum Press: New York, 1993; Vol. 13, pp 151−218.
(87) Symons, M. C. R.; Petersen, R. L. *Proc. R. Soc. London B* **1978**, *201*, 285−300.
(88) Davydov, R. M. *Biofizika* **1980**, *25*, 203−207.
(89) Kappl, R.; Höhn-Berlage, M.; Hüttermann, J.; Bartlett, N.; Symons, M. C. R. *Biochim. Biophys. Acta* **1985**, *827*, 327−343.
(90) Leibl, W.; Nitschke, W.; Hüttermann, J. *Biochim. Biophys. Acta* **1986**, *870*, 20−30.
(91) Davydov, R.; Kappl, R.; Hutterman, R.; Peterson, J. *FEBS Lett.* **1991**, *295*, 113−115.
(92) Davydov, R.; Kuprin, S.; Graslund, A.; Ehrenberg, A. *J. Am. Chem. Soc.* **1994**, *116*, 11120−11128.
(93) Davydov, R.; Valentine, A. M.; Komar-Panicucci, S.; Hoffman, B. M.; Lippard, S. J. *Biochemistry* **1999**, *38*, 4188−4197.

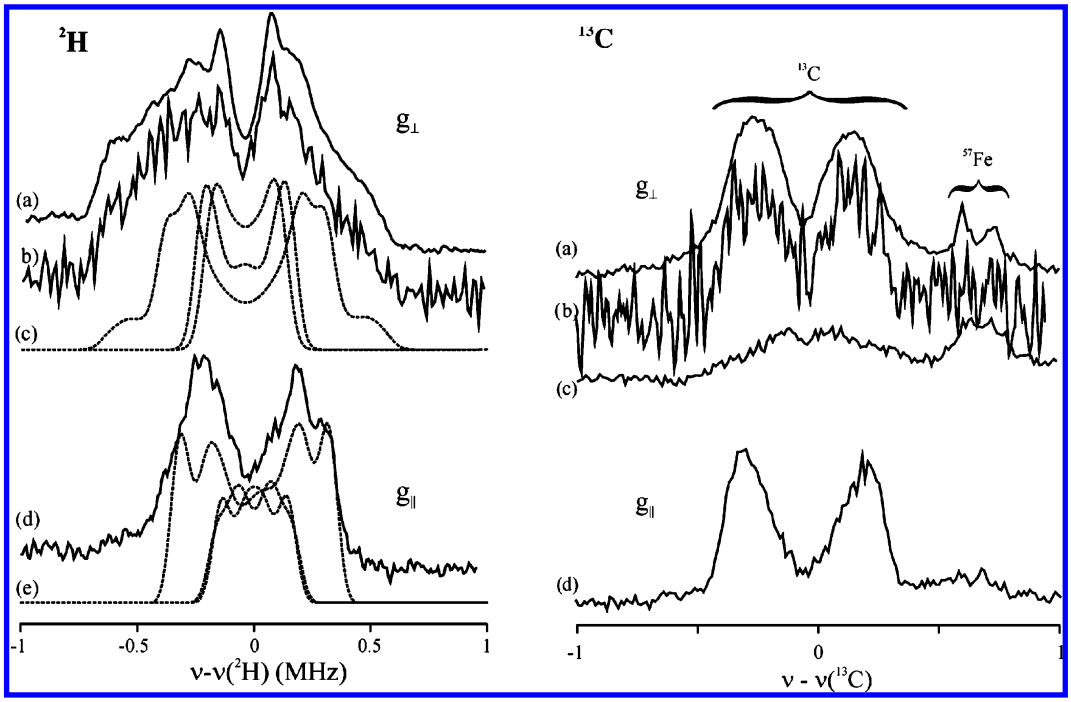

Figure 13. (Left) 35-GHz Mims pulsed-ENDOR spectra of PFL-AE with methyl-D_3 AdoMet. (a,d) photoreduced sample, (b) cryoreduced sample. The spectra at $g_\perp$ have been scaled to the height of the natural-abundance ^{57}Fe peaks visible to higher frequency of the ^{13}C signals. Conditions: $T = 2$ K, $\nu_{MW} = 34.8$ GHz, microwave pulse lengths = 80 ns, $\tau = 456$ ns, RF pulse length = 60 μs, repetition rate = 30 Hz. Each spectrum consists of 256 points with each point being an average of 240−300 transients. (c,e) Simulations (- - -) with dipolar **A** tensors. Closest ^{2}H: $T = 0.6$ MHz (corresponding to $R = 3.1$ Å for $K = 1.0$), $\alpha = \beta = 30°$, $\gamma = 0°$; $P = 0.1$ MHz, $\alpha = \beta = \gamma = 0°$. More distant methyl deuterons: $r\mathrm{Fe_k}-D = 4.7$ Å; representative value of $K = 1.6$; angles tetrahedrally disposed; orientations $\alpha = 19°$, $\beta = 20°$, $\gamma = 0$ and $\alpha = 30°$, $\beta = 54°$, $\gamma = 0$; quadrupole as above. Mims suppression effects included. (Right) 35-GHz Mims pulsed-ENDOR spectra of PFL-AE (a) with methyl-^{13}C AdoMet photoreduced at $g_\perp$, (b) with methyl-^{13}C AdoMet irradiated at 77 K at $g_\perp$, and (c) with natural-abundance ^{13}C -AdoMet at $g_{||}$. Experimental conditions as for left panel except that $\tau = 600$ ns and number of transients = 600. Reprinted from ref 48 with permission.

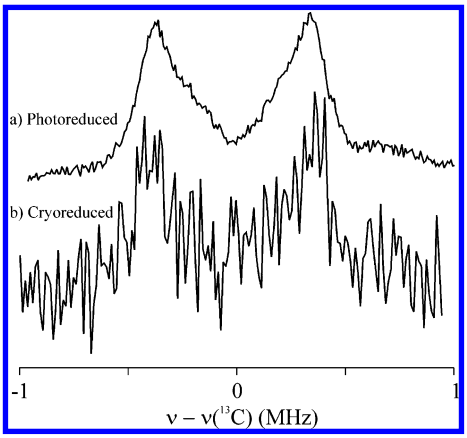

Figure 14. 35-GHz Mims pulsed ENDOR spectra of PFL-AE with carboxy-^{13}C−SAM at $g_\perp$: (a) photoreduced, (b) γ-irradiated at 77 K. Conditions: $T = 2$ K, $\nu_{MW} = 34.8$ GHz, microwave pulse lengths = 80 ns, $\tau = 562$ ns, RF pulse length = 60 ms.

tion geometry is the same in both the oxidized and reduced states of the [4Fe−4S] cluster.[48] The ENDOR spectrum of $[4Fe-4S]^{2+}_{RED}$−PFL-AE in the presence of carboxyl-^{13}C−SAM is also indistinguishable from that of the $[4Fe-4S]^{+}$−PFL-AE complex, thereby confirming that the geometry of binding of SAM to the [4Fe−4S] cluster of PFL-AE is the same in both the oxidized and reduced states of the cluster (Figure 14, Chart 1). ENDOR spectroscopy provided the first detailed insight into the interaction of SAM with the [4Fe−4S] cluster of a radical-SAM enzyme (Chart 1).[48,49] The mode of interaction elucidated via ENDOR spectroscopy, with methionine chelation of the unique site iron and orbital overlap with the sulfonium, was completely unprecedented and largely unexpected. The results suggest that the site-differentiated [4Fe−4S] cluster serves two key roles in catalysis: as an anchor, to coordinate the methionine moiety of SAM and thereby hold it in position, and as a catalyst, to promote reductive cleavage of the sulfonium S−C(5′) bond. Recently, several X-ray crystal structures of other members of the radical-SAM superfamily have been published, and in each case, these structures support our ENDOR results in terms of SAM coordination to the unique site of the [4Fe−4S] cluster.[50−52] The unique site therefore appears to be conserved throughout this superfamily for its essential role in coordinating the methionine moiety of SAM prior to reductive cleavage to generate the 5′-deoxyadenosyl radical intermediate.

A Mechanistic Proposal for PFL-AE and the Radical-SAM Enzymes

Taken together, the spectroscopic results presented herein provide significant insight into the mechanism by which PFL-AE, and more generally, all of the radical-SAM enzymes, initiate radical catalysis using an iron−sulfur cluster and *S*-adenosylmethionine (Scheme 3). As illustrated through EPR-detected single-turnover experiments, PFL-AE utilizes a reduced $[4Fe-4S]^{+}$ cluster in catalysis, and this cluster is the source of the electron required for reductive cleavage of SAM and subsequent generation of the glycyl radical in PFL.

Scheme 3. Proposed Mechanism for Iron−Sulfur Cluster and SAM-Mediated Radical Generation Catalyzed by PFL-AE

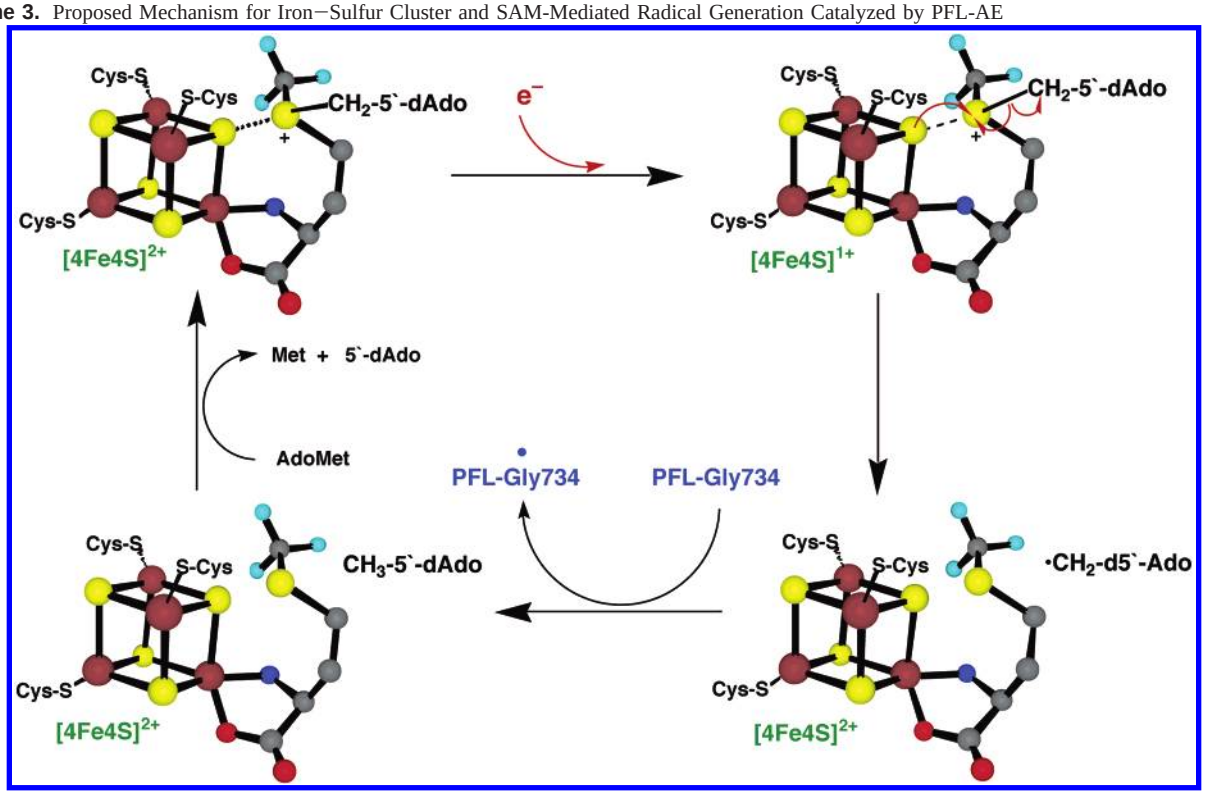

Mössbauer spectroscopy was used to identify a unique iron site in the [4Fe−4S] cluster of PFL-AE, and ENDOR spectroscopy showed that SAM coordinates to this unique iron via a classic five-member amino acid chelate ring in both the oxidized $[4Fe-4S]^{2+}$ and reduced $[4Fe-4S]^{+}$ states. ENDOR spectroscopy also demonstrated the close proximity of the sulfonium moiety to the cluster in both oxidation states.

On the basis of these observations, we propose a mechanism, outlined in Scheme 3, in which SAM binds to the oxidized $[4Fe-4S]^{2+}$ cluster of PFL-AE via coordination of the unique site, which puts the sulfonium in orbital overlap with one of the μ_3-bridging sulfides of the $[4Fe-4S]^{2+}$ cluster. One-electron reduction (mediated by reduced flavodoxin in vivo) provides the reduced $[4Fe-4S]^{+}$ cluster complexed to SAM. This $[4Fe-4S]^{+}$−SAM complex is stable in the absence of the substrate PFL; however, in the presence of PFL, inner-sphere electron transfer from the $[4Fe-4S]^{+}$ cluster to the sulfonium of SAM initiates homolytic S−C(5′) bond cleavage. The resulting methionine is left bound to the unique site of the oxidized $[4Fe-4S]^{2+}$ cluster, while the adenosyl radical intermediate abstracts the pro-*S* H from G734 of PFL. The catalytic cycle is completed upon displacement of methionine and 5′-deoxyadenosine with an *S*-adenosylmethionine cosubstrate. It is of interest to note that recent synthetic models of the radical-SAM enzymes based on site-differentiated [4Fe−4S] clusters have provided evidence for reductive cleavage of sulfonium moieties by reduced [4Fe−4S] clusters, although a stable synthetic cluster−sulfonium complex has not yet been reported.[94,95]

Concluding Remarks

The past 10 years have seen an explosion in interest in the enzymes now known to comprise the radical-SAM superfamily. These enzymes catalyze a diverse set of reactions, all of which are initiated by H atom abstraction. The evidence for adenosyl radical intermediates in some of these reactions led to early speculation of similarities to B_{12}-catalyzed radical reactions, the classic example of adenosyl-radical-mediated reactions in biology. However, the evidence to date points to novel chemistry utilized by the radical-SAM enzymes to generate adenosyl radical intermediates. This chemistry has at its core the use of a site-differentiated [4Fe−4S] cluster to coordinate and activate *S*-adenosylmethionine for reductive cleavage. Although many questions remain regarding the detailed mechanisms of these fascinating enzymes, it is clear that these ubiquitous enzymes are revealing new insights into the chemistry of iron−sulfur clusters.

Materials and Methods

General. All procedures were carried out under anaerobic conditions in a glovebox (Mbraun or Vacuum Atmospheres) or in a Coy chamber (Coy Laboratories) unless otherwise stated.

Proteins and Substrates. PFL-AE was overexpressed and purified as previously described.[37,48] Labeled *S*-adenosylmethionines were synthesized using AdoMet synthetase as previously described.[48,49] PFL-AE samples for photoreduction and for cryoreduction were prepared as previously described.[48,49]

Assay for PFL-AE and PFL activity. Inactive PFL (200 μM) was incubated with PFL-AE (generally 0.04−1 μM), 5-deazariboflavin (200 μM), and SAM (0.2 mM) in buffer containing Tris-Cl (50 mM, pH 8) and NaCl, and the mixture was illuminated at 25

(94) Daley, C. J. A.; Holm, R. H. *Inorg. Chem.* **2001**, *40*, 2785−2793.
(95) Daley, C. J. A.; Holm, R. H. *J. Inorg. Biochem.* **2003**, *97*, 287−298.

°C with a 500-W halogen lamp for varying periods of time. At given time points, EPR spectra were recorded at 60 K to monitor production of the glycyl radical. Double integration of the EPR spectra and comparison to a standard curve[96] provides a quantitative measure of the glycyl radical produced, and thus a rate of glycyl radical production by PFL-AE. Activated PFL was assayed for enzymatic activity as previously described.[37]

Photoreduction of PFL-AE. To purified PFL-AE in buffer containing 50 mM TrisCl pH 8.0 and 200 mM NaCl were added glycerol (to 20% w/v), DTT (1 mM), and 5-deazariboflavin (200 μM). The samples were placed in an ice−water bath 5 cm from a 500-W halogen lamp. Illumination was initiated, and overheating of the samples was avoided by replenishing the ice−water bath. At specified times, samples were removed from illumination and frozen in liquid nitrogen for analysis by EPR spectroscopy. For re-illumination of single-turnover samples, the samples containing PFL-AE, SAM, 5-deazariboflavin, and PFL were thawed and illuminated as above for 1 h.

EPR Spectroscopy. EPR measurements were obtained at the X-band on a Bruker ESP300E spectrometer equipped with a liquid He cryostat and a temperature controller from Oxford Instruments.

ENDOR Spectroscopy. Pulsed ENDOR spectra were collected on a spectrometer described earlier,[97] equipped with a helium immersion dewar for measurements at ~2 K. ENDOR measurements employed either the Mims pulse sequence ($\pi/2-\tau-\pi/2-T-\pi/2-\tau-$echo, where the RF was applied during the interval T) for small hyperfine couplings or the Davies pulse sequence ($\pi-T-\pi/2-\tau-\pi-\tau-$echo) for large couplings.

For a nucleus (N) of spin $I = {}^1/_2$ (^{13}C, ^{1}H) interacting with an $S = {}^1/_2$ paramagnetic center, the first-order ENDOR spectrum for a single molecular orientation is a doublet with frequencies (ν_+/ν_-) given by

$$\nu_\pm = \nu_N \pm A/2 \tag{1}$$

where ν_N is the Larmor frequency and A is the orientation-dependent hyperfine constant. For systems with $I \geq 1$, the first-order ENDOR resonance condition can be written as

$$\nu_\pm(\pm) = \nu_D \pm \frac{A}{2} \pm \frac{3P}{2} \tag{2}$$

where P is the orientation-dependent quadrupolar splitting. This is the case with ^{2}H, ^{14}N, and ^{17}O in this report.

For a nucleus with hyperfine coupling A, Mims pulsed ENDOR has a response R that depends on the product $A\tau$ according to the equation

$$R \sim [1 - \cos(2\pi A\tau)] \tag{3}$$

This function has zeroes, corresponding to minima in the ENDOR response (hyperfine "suppression holes"), at $A\tau = n$, $n = 0, 1, ...$, and maxima at $A\tau = (2n + 1)/2$, $n = 0, 1, ...$[98,99] The "holes" at $A = n/\tau$, $n = 1, 2, 3, ...$, can be adjusted by varying τ. However, the "central", $n = 0$, hole at $\nu = \nu_N$ persists regardless. This can be of significance in distinguishing a tensor that is dominated by anisotropic interactions from one that is dominated by isotropic ones. The latter would never give rise to ENDOR intensity near ν_N, whereas the former does for certain orientations. The effect of the $n = 0$ Mims hole is to diminish the differences between the two cases.

IC0484811

(96) Aasa, R.; Vänngård, T. *J. Magn. Reson.* **1975**, *19*, 308−315.
(97) Davoust, C. E.; Doan, P. E.; Hoffman, B. M. *J. Magn. Reson.* **1996**, *119*, 38−44.
(98) Mims, W. B. *Proc. R. Soc. London* **1965**, *283*, 452−457.
(99) Mims, W. B. In *Electron Paramagnetic Resonance*; Geschwind, S., Ed.; Plenum Press: New York, 1972.